



Diagnosis of Alzheimer's disease based on regional attention with sMRI gray matter slices

Yanteng Zhang^a, Qizhi Teng^{a,*}, Yuyang Liu^b, Yan Liu^c, Xiaohai He^a

^a College of Electronics and Information Engineering, Sichuan University, Chengdu, Sichuan 610065, China

^b Information School, The University of Sheffield, Sheffield S10 2TN, UK

^c Department of Neurology, Chengdu Third People's Hospital, Chengdu, Sichuan 610031, China

ARTICLE INFO

Keywords:

Deep learning
Attention mechanism
Alzheimer's disease
sMRI gray matter slice

ABSTRACT

Background: Alzheimer's disease (AD) is the most common symptom of aggressive and irreversible dementia that affects people's ability of daily life. At present, neuroimaging technology plays an important role in the evaluation and early diagnosis of AD. With the widespread application of artificial intelligence in the medical field, deep learning has shown great potential in computer-aided AD diagnosis based on MRI.

New method: In this study, we proposed a deep learning framework based on sMRI gray matter slice for AD diagnosis. Compared with the previous methods based on deep learning, our method enhanced gray matter feature information more effectively by combination of slice region and attention mechanism, which can improve the accuracy on the AD diagnosis.

Results: To ensure the performance of our proposed method, the experiment was evaluated on T1 weighted structural MRI (sMRI) images with non-leakage splitting from the ADNI database. Our method can achieve 0.90 accuracy in classification of AD/NC and 0.825 accuracy in classification of AD/MCI, which has better diagnostic performance and advantages than other competitive single-modality methods based on sMRI. Furthermore, we indicated the most discriminative brain MRI slice area determined for AD diagnosis.

Comparison with existing methods: Our proposed method based on the regional attention with GM slice has a 1%–8% improvement in accuracy compared with several state-of-the-art methods for AD diagnosis.

Conclusions: The results of experiment indicate that our method can focus more effective features in the gray matter of coronal slices and to achieve a more accurate diagnosis of Alzheimer's disease. This study can provide a more remarkably effective approach and more objective evaluation for the diagnosis of AD based on sMRI slice images.

1. Introduction

Alzheimer's disease (AD) is a progressive and irreversible brain disease, which is the most common cause of dementia. With the gradual progress of AD, neurons in a wide area of the brain are irreversibly damaged, and the symptoms mainly include memory loss, cognitive decline, and so on, which eventually lead to the loss of daily activity capacity (Barker et al., 2015). This has taken a heavy toll on the families of AD patients and on the whole society. At the same time, AD patients often show abnormal behavior and psychological problems, which bring additional care difficulties to the caregivers. At present, about 90 million people in the world have been diagnosed with AD, and over 65 years old will greatly increase the probability of suffering from AD (Alzheimer's

Association, 2017). With the aggravation of global aging, the number of AD patients worldwide is expected to reach 300 million by 2050 (Zhan et al., 2015). Although many institutions have conducted relevant clinical studies, so far the existing AD drugs have only alleviated symptoms or slowed their progress (Servick, 2019). In the preclinical phase of AD, people often experience a measurable status of cognitive ability, which does not significantly affect daily life, called mild cognitive impairment (MCI) between the stage of normal control (NC) and AD, but an average of 32% of MCI patients develop AD related symptoms within five years (Roberts and Knopman, 2013). Therefore, early diagnosis of AD has clinical significance and necessity for preventing and interfering with its progress, and it can also provide better opportunities for patients to fight.

* Corresponding author.

E-mail address: qzteng@scu.edu.cn (Q. Teng).

<https://doi.org/10.1016/j.jneumeth.2021.109376>

Received 15 June 2021; Received in revised form 30 September 2021; Accepted 1 October 2021

Available online 8 October 2021

0165-0270/© 2021 Elsevier B.V. All rights reserved.

The clinical diagnosis of AD is mainly completed by comprehensive assessment such as physiological and neurobiological examination and mini mental state examination (MMSE) (Marco et al., 2011). Among them, neuroimaging technology has been widely used to discover related biomarkers in the human brain for diagnosing AD and MCI. sMRI can provide detailed images of the brain's internal structure, help us understand changes in the brain's anatomical structure and function associated with AD, and play an important role in the evaluation and diagnosis of AD (Jr et al., 2011). In recent years, with the identification of AD biomarkers, structural changes of the gray matter atrophy proposed in many studies can be seen obviously in MCI and AD patients (Fan et al., 2006; Ahmed et al., 2015). These structural changes are reflected in the shrinkage or thinning of the cortical thickness and the atrophy of the hippocampus in brain through the sMRI. To this end, many studies have focused on analyzing shrinkage patterns and extracting features from sMRI images in spatial domains for application in the field of AD diagnosis (Liu et al., 2014; Wood et al., 2019).

Convolutional Neural Network (CNN), as a powerful method in deep learning, uses image features and spatial context to generate feature hierarchies through neighborhood information, which can be applied in image-related classification tasks (Lecun et al., 2015; Hou et al., 2016). With the widespread application of artificial intelligence in the medical field, various 2D and 3D convolutional neural network architectures perform well in the diagnosis of cognitive diseases. Especially deep learning has shown great potential in computer-aided AD and MCI diagnosis based on MRI data (Zhang et al., 2020). Recently, many researches use 2D slices extracted from 3D MRI volume as datasets, and realize the diagnosis of AD based on CNNs. Another advantage is the multiple slices extracted from 3D MRI can increase the number of training samples. Hon (Hon and Khan, 2017) trained VGG and Inception networks via transfer learning based on MRI slices, and achieved considerable classification effect on OASIS dataset. Farooq (Farooq et al., 2017) carried out classification experiments on ADNI datasets based on CNNs, and obtained outstanding prediction accuracy of multiple categories of Alzheimer's disease. To distinguish different stages of MCI from the NC group, Wu (Wu et al., 2018) employed GoogleNet and CaffeNet with pretrained ImageNet via transfer learning to explore and evaluate in multiple classifications. Korolev (Korolev et al., 2017) demonstrated the classification performance of AD/MCI/NC based on residual and plain 3D convolutional neural network architectures using sMRI scans. Valliani (Valliani and Soni, 2017) evaluated on the ADNI imaging data based on the deep residual network, which shows that the pretrained residual network is effective for the diagnosis of Alzheimer's disease.

In the neural network-based diagnosis of AD, the patients in the dataset are usually classified as Alzheimer's disease, mild cognitive impairment and normal control. Although many previous studies have high accuracy in AD classification based on sMRI slice images, we found that the validity of these results was questioned (Wen et al., 2020). In brain MRI datasets, many studies randomly divided brain MRI slices into training and test set (Hon and Khan, 2017; Farooq et al., 2017; Wu et al., 2018; Korolev et al., 2017), but this implied situation must be that the MRI scan results of the same patient may exist in both the training set and test set. That is to say, at the time of test, the patient's MRI image has appeared in the process of training, which is called data leakage (Wen et al., 2020).

The main contributions of this study are as follows. First, we divide the training set and the test set without leakage, so as to effectively evaluate the classification performance of our proposed method. The result(without data leakage) of AD diagnosis is that no previous or subsequent patient information is given. Secondly, from a clinical point of view, it is particularly important to understand which parts of the brain are pathological and the relationship between different brain regions and symptom observation. Based on this mechanism, we recognize those parts of the brain affected by pathological diseases as the diagnostic criteria. Through the gray matter to evaluate and represent

regional abnormalities to determine the clinical status of the brain within the range of AD progression, and propose a diagnosis method combined with regional GM features based on CNN structure. Furthermore, the diagnosis of AD using 2D MRI slice has the advantage of expanding the amount of data. Finally, we carried out classification experiments based on our proposed network. Compared with several other single-modality methods based on ADNI sMRI data, our proposed method has better performance in classification of Alzheimer's disease.

2. Materials

2.1. Datasets

All the neuroimaging data we used in this work were obtained from the Alzheimer's disease neuroimaging Initiative (ADNI) database (Peterson et al., 2010). ADNI is a campaign launched in North America in 2003 to provide magnetic resonance imaging, positron emission tomography, clinical neurometry and other biomarkers. We used T1 weighted sMRI from ADNI baseline, the sMRI images are obtained using MPRAGE sequence (Jack et al., 2010) and a total of 496 subjects are included in our experiment. The subjects included men and women, aged between 65 and 85. Specifically, there are 139 subjects with AD, 198 subjects with MCI and 159 subjects with NC. Table 1 summarized the demographic information of the sMRI data used in our study.

2.2. Data preprocessing

In our data preprocessing, we divide the sMRI dataset according to the subject's number. The first n-1 number of the subjects data is used for network training, and the data after n number is used for network validation and testing. We divide the number of subjects into a ratio of 7:1:2. In this way, MRI slices from the same subject are not assigned to the training set, validation set and test set at the same time. We used conventional procedures for MRI image preprocessing, anterior commissure(AC) correction, skull stripping, registration and gray matter (GM) extraction. Specifically, the following steps are used to preprocess the data. AC correction is performed by the Matlab tool SPM. The brain tool FSL bet (Woolrich et al., 2009) is used to separate non-brain tissue from the whole head imaging, and the FSL flirt performs affine registration in MNI152 space to align the image with the standardized template (Jenkinson et al., 2002; Klein et al., 2009). The volume of each processed sMRI is $121 \times 145 \times 121$, and then the Matlab tool CAT12 is used to extract GM from the preprocessed sMRI volume, and the size of GM slice is 121×121 . The above data preprocessing is performed in MNI space. We checked the quality of preprocessed images and excluded some failed images. In view of the influence of brain atrophy in the process of Alzheimer's disease, we use GM features for diagnosis. The data preprocessing steps are shown in Fig. 1.

3. Methods

In this part, we will mainly describe the structure and framework of the proposed network. Our method is inspired by the following two aspects. Firstly, in order to improve the diagnostic accuracy, especially in the stages of Alzheimer's disease progression, the diagnostic network should be sensitive to the slight changes in brain volume. For patients with AD, the atrophy area is usually concentrated in the entorhinal cortex and hippocampus, which can reflect the degree of atrophy more

Table 1
the demographic information of the sMRI data used in our study.

	AD	MCI	NC
Number of Subjects	139	198	159
Gender(Male/Female)	78/61	115/83	77/82
Age (Mean + SD)	75.4 ± 7.5	75.7 ± 6.5	76.0 ± 5.0

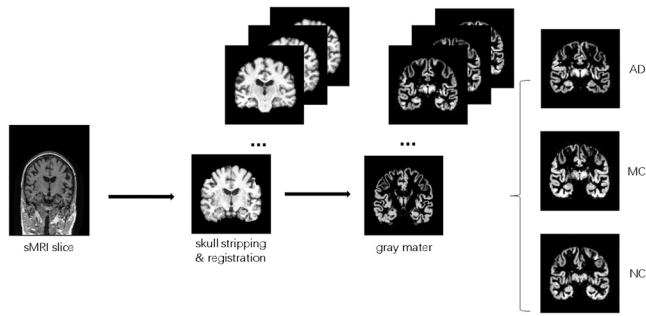


Fig. 1. the preprocessing steps of sMRI data.

visually on the coronal plane of sMRI, as shown in the Fig. 2. For this reason, we chose GM slice of coronal section as the source data. Secondly, we know that most of the regional information in sMRI image has nothing to do with the disease, especially for the very similar images between brain individuals, which makes the diagnosis of AD more difficult. Therefore, we use enhanced sMRI GM regional feature information to realize the diagnosis of AD based on convolutional neural network. Finally, we give the training and evaluation process of our proposed network.

3.1. Network structure

Residual network (Valliani and Soni, 2017; He et al., 2016) has been proved to be highly effective in image classification and related recognition tasks. For the classification method based on 2D MRI slices, we use the improved framework tresnet (Ridnik et al., 2020) of residual network. The frame was fine tuned by combining with subtle changes, and the MRI image features were associated with the clinical diagnosis of cognitive status. In order to improve the effectiveness of the regional information of the input image, we use GM regional area as input of the neural network. Due to the approximate symmetry of the coronal slice image structure, we divide each slice into four identical regions as the input of the network, and the resolution of the GM regional information is not reduced. In order to generate more sensitive feature responses to GM striation and hippocampal changes, then we introduce attention mechanism based on these four parts of sMRI regions in our network to mine the potential features.

3.2. Spacetodepth block

The mechanism of convolution layer in neural network is to rapidly reduce the input resolution to obtain feature maps. For example, the convolution layer of ResNet is composed of a conv 7×7 with a stride of 2

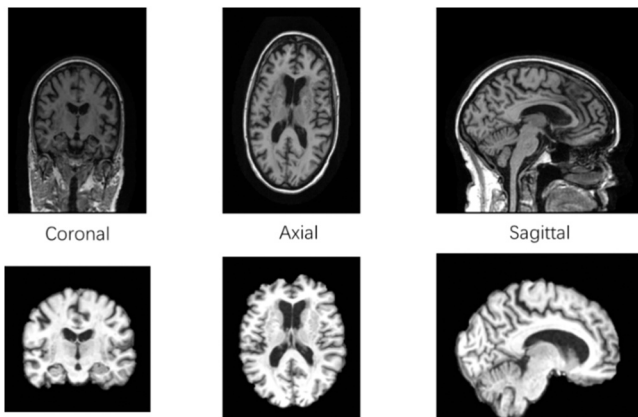


Fig. 2. the axial, coronal, and sagittal view of the brain sMRI slice.

and a max pooling layer, which reduces the input resolution by 4 times (120→30). In contrast, the mechanism of spacetodepth block is more elaborate, which can minimize the loss of local information as much as possible. The spacetodepth block, as shown in Fig. 3, which rearranges blocks of spatial image into depth block and improves the resolution of image input. Specifically, we use the spacetodepth block to divide each MRI slice image into four pieces before the first convolution layer in our network, so as to improve the significance of sMRI regional feature information, and the spacetodepth block is followed by a simple 1×1 convolution to match the number of channels required.

3.3. Attention mechanism

Attention mechanism is widely used in various tasks based on neural network model. Its essence is a series of attention distribution weight parameters, which can be used to enhance the important information of processing objects and suppress some irrelevant details. For this reason, the attention mechanism is introduced to excavate the potential features of the corresponding ROI in gray matter slice. In our network, the attention mechanism is inspired by Squeeze-and-Excitation block (Jie et al., 2020) and the mechanism of channel attention module is shown in Fig. 4. For an input graph X with C channel, the action will be completed in the following steps.

First of all, the features are compressed in the spatial dimension, and the two-dimensional features of each channel are converted into real numbers with a certain global receptive field, the output dimension is consistent with the number of the input channels. This process can be realized by global pool, the corresponding operation equation is given as follows.

$$Z_c = \frac{1}{H \times W} \sum_i^H \sum_j^W X_c(i, j)$$

Where H and W are the height and width of each feature graph, and C is the number of feature channels.

Based on the correlation between feature channels, a set of compressed real numbers is used to map each channel, and a new weight is generated to represent the importance of each channel. The weight distribution of these channels can be achieved via 1×1 convolution, and the corresponding calculation formula is as follows.

$$SC = \delta(\text{conv}(ZC))$$

Where δ is the Sigmoid activation function.

In the previous step, the new weight reflects the importance of each feature channel. Then the original features are weighted to each channel by multiplication to complete the redistribution in channel dimension. The transformation mapping XC to $X'C$ of input features can be expressed as follows.

$$X'_C = S_c \otimes X_c$$

In this way, the feature map XC is transformed into a new feature map $X'C$ with reweighted channel information. By learning the feature weights according to the loss of the network, the effective feature map can be with larger weight and the ineffective feature map with smaller weight. In our network structure, we utilized the self attention with every 4 regions ($r = 4$) of the input GM slice image, the input process of GM slice based on attention mechanism and the network framework is shown in Fig. 5.



Fig. 3. the architecture of the spacetodepth block.

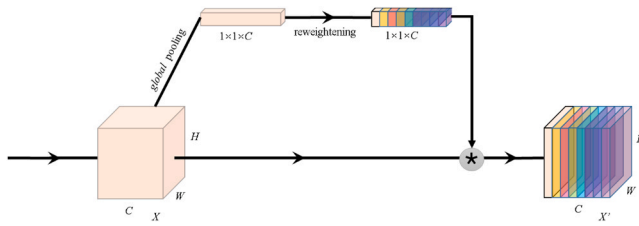


Fig. 4. the mechanism of channel attention module in our network.

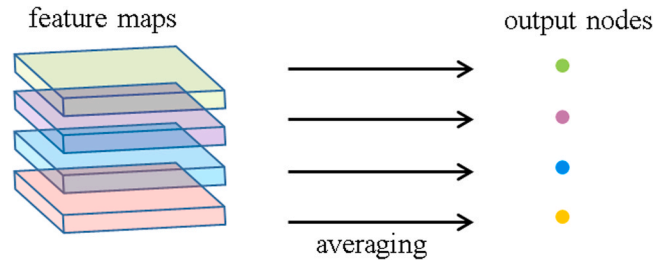


Fig. 6. the mechanism of global average pool layer.

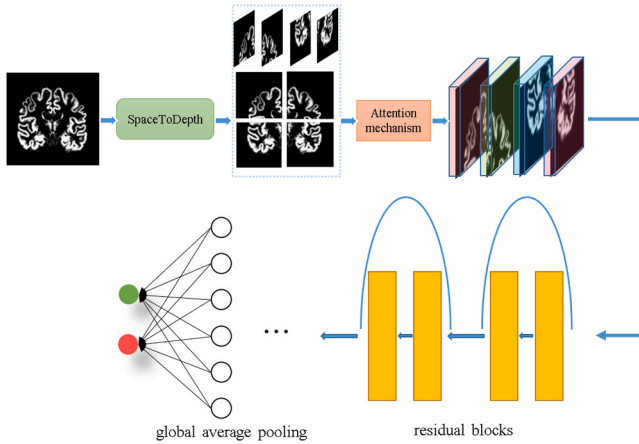


Fig. 5. the framework of our proposed AD diagnosis network.

The overall structure of our AD diagnosis network is shown in Table 2, which including the channels, output size and the number of residual layer in each stage. The residual layer contains multiple basicblocks and bottlenecks (He et al., 2016), adding the shortcut connection for output summation of convolution layers, and the classification is implemented through a global average pool layer (Min et al., 2014) and softmax at the end of the network.

The global average pooling layer reduces the number of parameters to achieve feature dimensionality reduction, replacing the traditional fully connected layer. As shown in Fig. 6, the global average pooling takes the last layer's feature map into an average value of the whole map, formed a feature node for each feature map, and composed these feature points into the final feature vector for calculation in softmax. The probability of classification output is obtained by softmax, and the calculation function of softmax for K categories is as follows:

$$\text{softmax}(z_j) = \frac{\exp(\frac{z_j}{T})}{\sum_{j=1}^K \exp(\frac{z_j}{T})}$$

4. Experimental results and discussion

In this section, we first describe the implementation details in our experiments. Then we explored the classification effect based on sMRI GM slice images, and gave the experimental classification results on the ADNI database. We considered classification tasks including AD and NC,

Table 2
The structure of our AD diagnosis network.

Layer	Output	Stride	Repeats	Channels
SpaceToDepth	60×60	–	1	48
Conv1×1		1	1	64
BasicBlock	60×60	1	3	64
BasicBlock	30×30	2	4	128
BasicBlock	15×15	2	11	1024
Bottleneck	7×7	2	3	2048
GlobalAvgPool	1×1	1	1	2048

MCI and NC, AD and MCI. To demonstrate the performance of our proposed method, we report three different indicators commonly considered in subject diagnosis, namely accuracy(ACC), sensitivity (SEN) and specificity(SPE). We compared and analyzed with the state-of-the-art methods based on sMRI data for AD diagnosis. In addition, in order to evaluate the impact of sMRI slices on the diagnosis of AD, we also carried out the corresponding slice area contrast experiments. Finally, we illustrated the most discriminative brain MRI slice area determined for AD diagnosis based our method.

4.1. Implementation details

For the sMRI GM 2D-slice experiments, we utilized the pretrained model of resnet on ImageNet to implement classification task of our network. In order to evaluate the performance of our proposed method, we trained our classification network model from scratch and the training setting of network is as follows. We use the stochastic gradient descent (Bottou, 2010) with learning rate is optimally set to 0.01. The cross entropy loss (Vincent et al., 2010) is used as the loss function and the hyperparameters are set with a weight decay of 0.0001 and a momentum of 0.9. In our deep neural network, the input image size is set to 120×120 . The results are obtained after each model has been trained for 40 epochs with a batch size of 16, and the valid loss no longer improved. Our network implemented using Pytorch (Kossaiifi et al., 2016) and performed on a Linux X86-64 computer machine with Intel (R) Xeon(R) CPU E5-2686 v4 @ 2.30 GHz, 32 GB of RAM and GeForce GTX 1080Ti.

4.2. Experimental results

According to the severity of hippocampus atrophy in the coronal plane, we selected the range of the 72–76th in the 145-dimension coronal slices of sMRI volume. The method based on slice images has the advantage of data augmentation. For this reason, we conducted classification experiments based on two groups of three consecutive MRI slices of each subject, and we also carried out based on all 5 slices. All test experiments use the 74th sMRI slice of the subject that is commonly included as the test data. Like most AD diagnosis studies without data leakage, we compared the accuracy, sensitivity and specificity of our proposed network on the classification tasks of AD/CN, AD/MCI and MCI/CN. First of all, Table 3 summarizes the experimental results of our method based on regional attention with GM slice.

Judging from the results of our experiments, the classification of AD/NC has an optimistic accuracy, of which 3 groups of experiments are all above 0.85. The accuracy based on 5-slice is slightly higher than that of 3-slice, achieved 0.90. We give the corresponding loss and valid accuracy curves in training step based on the 72–76th slices, as shown in Fig. 7. While the corresponding SEN and SPE is 0.928 and 0.875, which indicates that the diagnosis of both AD and NC has high accuracy. The accuracy of binary classification of MCI categories is decreased, and the accuracy of AD/MCI classification is better than that of MCI/NC. The results indicate that for MRI GM images, the feature information of MCI is more obvious than AD and more similar to NC. Our network is more

Table 3
the classification results based on regional attention mechanism.

Slice	AD/NC			AD/MCI			MCI/NC		
	ACC	SEN	SPE	ACC	SEN	SPE	ACC	SEN	SPE
72–74	0.883	0.892	0.875	0.793	0.750	0.828	0.671	0.800	0.531
74–76	0.866	0.821	0.906	0.777	0.607	0.914	0.656	0.742	0.562
72–76	0.900	0.928	0.875	0.825	0.785	0.857	0.626	0.828	0.406

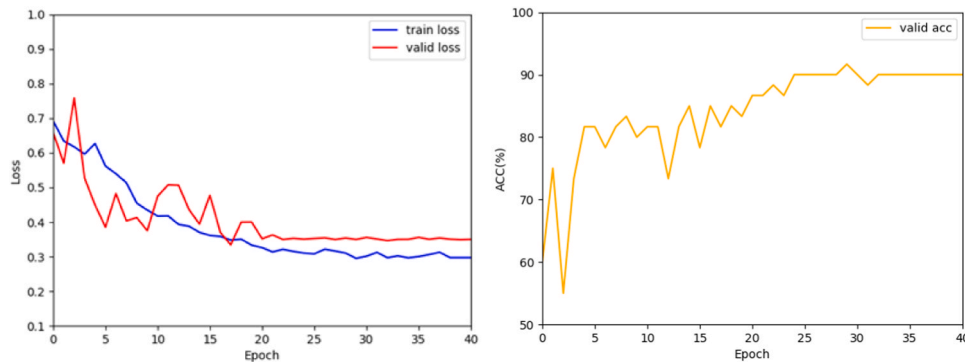


Fig. 7. the loss and valid accuracy curves in training step of the AD/NC classification.

sensitive to AD/MCI classification than MCI/NC.

In the AD/MCI classification task, the accuracy of 5-slice is higher than that of 3- slice. The accuracy of 5-slice group is 0.825, the sensitivity and specificity are 0.785 and 0.857 respectively, indicating that more AD symptoms are diagnosed as MCI. In classification of MCI/NC, the accuracy of the two 3-slice groups is relatively higher. The sensitivity and specificity of MCI based on the 72–74th slices are 0.80 and 0.531 respectively, indicating that more NC symptoms are misdiagnosed as MCI symptoms. In the AD categories classification with more obvious features, the data volume of 5-slice is more conducive to the training of classification network, while in the MCI/NC classification with similar features, the increase of slices is not conducive to the improvement of network classification performance. We conclude that in the diagnosis of similar symptoms, the higher the dimension of the slice will bring more information noise, which is not conducive to the improvement of classification accuracy. Among the classification tasks of two 3-slice groups, the accuracy of the 72–74th slices is better. And the classification accuracy of AD/NC, AD/MCI and MCI/NC are 0.883, 0.793 and 0.671 respectively, which is relative higher to the accuracy of the 74–76th slices. It also indicates that the 72–74th slices provide the main contribution in the 5-slice area.

Secondly, we still divide the GM slice into 4 equal regions as the network input, eliminating the role of attention mechanism for classification experiments, and the results is shown in Table 4. Judging from the comparison of the classification results in Fig. 8, the accuracy without attention mechanism (AM) is reduced to a certain extent, but the overall trend has not changed much. This shows that our proposed regional attention method is effective in improving the diagnosis of AD.

In order to compare the effect of the attention mechanism with different slice numbers on the diagnosis of AD, we also used every 8 and every 16 regions of GM slices based on the 72–76th as the network input,

Table 4
the classification results without regional attention mechanism.

Slice	AD/NC			AD/MCI			MCI/NC		
	ACC	SEN	SPE	ACC	SEN	SPE	ACC	SEN	SPE
72–74	0.850	0.857	0.843	0.777	0.678	0.857	0.656	0.714	0.593
74–76	0.833	0.857	0.812	0.746	0.642	0.828	0.641	0.685	0.593
72–76	0.883	0.892	0.875	0.761	0.714	0.800	0.611	0.714	0.500

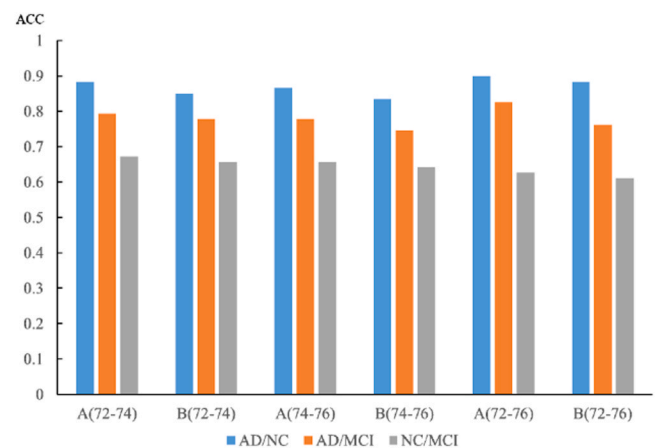


Fig. 8. comparison of the classification accuracy (A including attention mechanism; B without attention mechanism).

and the classification accuracy is shown in Fig. 9. It is not difficult to see from the figure that the overall classification effect trend has not changed much, the accuracy of AD/NC classification is still the best. In various classification tasks, the attention mechanism based on every 4 slice regions ($r = 4$) works best, and as parameter r multiples, its classification accuracy decreases slightly.

4.3. Discussion

This research includes several major contributions. First of all, we conducted a brief overview and clarified the data leakage problems in

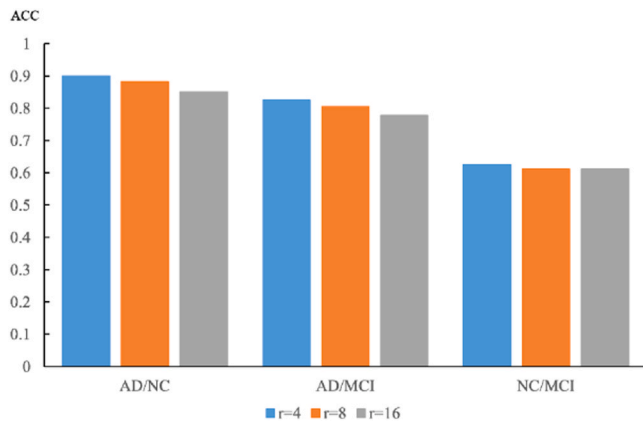


Fig. 9. comparison of the classification accuracy with different numbers of slice regions.

some studies. Secondly, we propose a neural network framework for repeatable evaluation of AD classification based on CNN using sMRI GM slice. Then we discussed the classification of AD based on several groups of GM slices, and indicated the diagnostic effect of GM slice on Alzheimer's disease. Finally, we compared the classification performance of several state-of-the-art methods for AD diagnosis based on sMRI data, which shows the effectiveness of our proposed method.

In the introduction of this paper, we point out the problem of data leakage in the existing research of AD diagnosis based on CNN methods. In some investigations (Wen et al., 2020), it is found that more than half of the studies may have data leakage. We list five cases of AD diagnosis studies based on sMRI data via deep learning, as shown in Table 5. Data leakage makes some test samples from the same subject appear in the training set, resulting in the classification accuracy is seriously high compared with most of the current cutting-edge methods. AD diagnosis based on these methods is not valid.

In order to verify the performance of our proposed method, we list several state-of-the-art methods of AD diagnosis based on sMRI data, as shown in Table 6. We selected studies that do not involve data leakage problem as much as possible, most of which mainly analyze AD/NC diagnosis. In the sMRI data based diagnosis of Alzheimer's disease, our proposed method based on the regional attention with GM slices has a 1%–8% improvement in accuracy compared with other single-modality methods. The 0.90 accuracy in classification of AD/NC is an outstanding performance on the non-leakage dataset, and it also has high sensitivity and specificity of AD/NC. As the training set of network, the number of subjects we used is relatively small. In our method, the results indicate that the combination of regional features and attention mechanism can reduce the interference of redundant information to a certain extent, retain more effective features, and achieve more effective diagnosis. In addition, GM features and slice selection also contribute to the classification effect. Therefore, the diagnostic accuracy of AD can be improved to some extent by attending GM feature information of sMRI.

In addition, we compared the results of some studies with MCI diagnosis, as shown in Table 7. In the classification of AD/MCI, our accuracy achieved 0.825, which is greatly improved compared with

Table 5
the accuracy of related studies based on sMRI data with leakage problem.

STUDY	AD/NC	AD/MCI	MCI/NC	APPROACH
Hon (Hon and Khan, 2017)	0.962			2D slice
Wang (Wang et al., 2017)			0.906	2D slice
Tien (Tien-Duong et al., 2018)	0.988	0.930	0.950	2D slice
Taqi (Taqi et al., 2018)	0.995			2D slice
Backstrom (Backstrom et al., 2018)	0.987			3D subject

Table 6
the AD/NC classification of studies based on sMRI data without leakage problem.

STUDY	ACC	SEN	SPE	SUBJECTS
ADERGHAL(2017) (Aderghal et al., 2017)	0.837	0.791	0.872	188AD, 228NC
FAN(2017) (Fan et al., 2017)	0.883	0.914	0.844	199AD, 229NC
KOROLEV(2017) (Korolev et al., 2017)	0.80	—	—	50AD, 61NC
VALLIANI(2018) (Valliani and Soni, 2017)	0.813	—	—	188AD, 299NC
BRÜNINGK(2020) (Brüningk et al., 2020)	0.880	0.890	0.90	—
WEN(2020) (Wen et al., 2020)	0.880	—	—	336AD, 330NC
OURS	0.90	0.928	0.875	139AD, 159NC

Table 7
the MCI classification of studies based on sMRI data without leakage problem.

STUDY	AD/MCI (ACC)	MCI/NC (ACC)	SUBJECTS
ADERGHAL (Aderghal et al., 2017)	0.665	0.649	188AD, 399MCI, 228NC
KOROLEV (Korolev et al., 2017)	0.64	0.56	50AD, 77MCI, 61NC
OURS	0.825	0.671	139AD, 198MCI, 159NC

other classification methods. In the classification of MCI/NC, it is not difficult to find that the classification performances of many methods are not optimistic. MCI is the manifestation of mild cognitive impairment, most of the patients are still in a status of cognitive lucidity, many MCI and normal cognitive patients have little difference. There are still some difficulties in the MCI diagnosis of single-modality methods based on MRI images, which need to be further combined and explored.

In this paper, for better diagnosis results of Alzheimer's disease, we indicated the specific area of the slice image for reference. Among the processed 145-dimension coronal slices, the slices of the 72–74th area are more important for the diagnosis of Alzheimer's disease, and the doctor can select the slices of this area for disease screening. We visualized a comparison of the original sMRI 72–74th slices of three symptoms shown in Fig. 10, and marked the main parts with obvious changes,

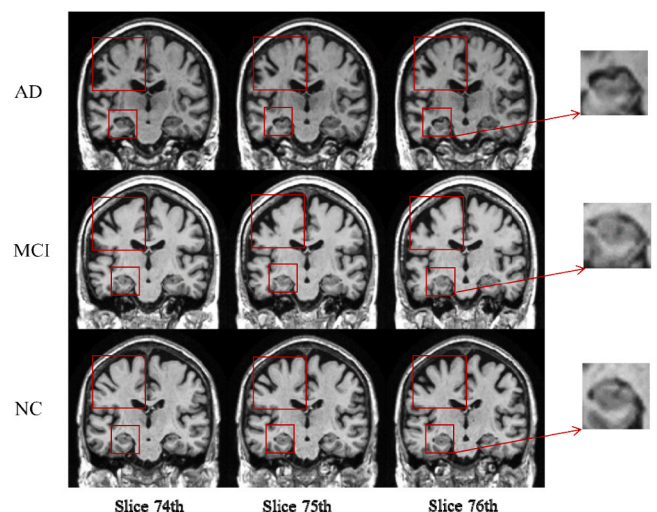


Fig. 10. images from left to right are the original sMRI 72–74th slices of three symptoms.

such as the hippocampus. In our experiments, it demonstrates that our method has high sensitivity and specificity for AD. Sensitivity index corresponds to the initial screening in the process of diagnosis, and it is a measure of missed diagnosis. Relatively, specificity is an important indicator for the diagnosis of disease. In addition, we can conclude sMRI GM slices are significant marker for preliminary screening in the diagnosis of Alzheimer's disease.

5. Conclusion

Based on the texture of sMRI gray matter images and the features of hippocampus structure, we proposed a deep learning method for AD diagnosis based on regional attention with gray matter slice. Our method can focus more effective features in the gray matter coronal image and to achieve a more accurate diagnosis of Alzheimer's disease. Furthermore, we explored the correlation between some slices of sMRI regions and AD diagnosis. To avoid the invalid AD diagnosis, in this study all the datasets are based on non-leakage splitting. Compared with some state-of-the-art methods for AD diagnosis based on sMRI data, our proposed method has better diagnostic performance and advantages. Many studies may cause misdiagnosis results due to splitting at the slice-level of sMRI data, thus we hope that this study can provide more objective assessment and further reference of AD diagnosis based on sMRI slice images.

CRedit authorship contribution statement

Yanteng Zhang: Writing – original draft, Methodology, Software. Qizhi Teng: Supervision, Funding acquisition. Yuang Liu: Writing – reviewing & editing, Investigation. Yan Liu: Formal analysis. Xiaohai He: Project administration.

Declaration of Competing Interest

The authors declare that they have no known competing financial interests or personal relationships that could have appeared to influence the work reported in this paper.

Acknowledgments

This work was supported in part by the National Natural Science Foundation of China [Grant No. 62071315], in part by Chengdu Major Technology Application Demonstration Project [2019-YF09-00120-SN].

References

Aderghal, K., Boissenin, M., Benois-Pineau, J., et al., 2017. Classification of sMRI for AD Diagnosis with Convolutional Neuronal Networks: A Pilot 2-D+ Study on ADNI[C]//Multimedia Modeling International Conference. Alzheimer's Association, 2017. 2017 Alzheimer's disease facts and figures. *Alzheimer's Dement.* 13 (4), 325–373.

Backstrom, K., Nazari, M., Gu, YH, et al., 2018. An efficient 3D deep convolutional network for Alzheimer's disease diagnosis using MR images. *Proceedings of the IEEE 15th International Symposium on Biomedical Imaging*, pp. 149–153.

Barker, W.W., Luis, C.A., Kashuba, A., Luis, M., Harwood, D.G., Loewenstein, D., Waters, C., Jimison, P., Shepherd, E., Sevush, S., Graff-Radford, N., Newland, D., Todd, M., Miller, B., Gold, M., Heilman, K., Doty, L., Goodman, I., Robinson, B., Pearl, G., Dickson, D., Duara, R., 2015. Relative frequencies of Alzheimer disease, Lewy body, vascular and frontotemporal dementia, and hippocampal sclerosis in the State of Florida Brain Bank. *Alzheimer's Dis. Assoc. Disord.* 16 (4), 203–212.

Ben Ahmed, O., Benois-Pineau, J., Allard, M., Ben Amar, C., Catheline, G., 2015. Classification of Alzheimer's disease subjects from MRI using hippocampal visual features. *Multimed. Tools Appl.* 74 (4), 1249–1266.

Bottou, L.éon, 2010. Large-scale machine learning with stochastic gradient descent. *Proceedings of Computational Statistics*. Springer, pp. 177–186.

Brünink, S.C., Hensel, F., Jutzeler, C.R., et al., 2020. Image analysis for Alzheimer's disease prediction: embracing pathological hallmarks for model architecture design [DB/OL]. arXiv:2011. 06531.

Fan, L., Cheng, D., Liu, M., et al., 2017. Alzheimer's disease classification based on combination of multi-model convolutional networks. *Proceedings of the IEEE International Conference on Imaging Systems and Techniques*.

Fan, Y., Shen, D., Gur, R.C., Gur, R.E., Davatzikos, C., 2006. COMPARE: classification of morphological patterns using adaptive regional elements. *IEEE Trans. Med. Imaging* 26 (1), 93–105.

Farooq, A., Anwar, S., Awais, M., et al., 2017. A deep CNN based multi-class classification of Alzheimer's disease using MRI. *Proceedings of the IEEE International Conference on Imaging Systems and Techniques*, pp. 1–6.

He, Kaiming, Zhang, Xiangyu, Ren, Shaoqing, et al., 2016. Deep residual learning for image recognition. *Proceedings of the IEEE Conference on Computer Vision and Pattern Recognition*, pp. 770–778.

Hon M., Khan NM. Towards Alzheimer's disease classification through transfer learning [C]//In Proceedings of the IEEE International Conference on Bioinformatics and Biomedicine. 2017, 1166–1169.

Hou L., Samaras D., Kurc T.M., et al. Patch-Based Convolutional Neural Network for Whole Slide Tissue Image Classification[C]//Proceedings of the IEEE Conference on Computer Vision and Pattern Recognition, 2016, 2424–2433.

Hu, J., Shen, L., Albanie, S., Sun, G., Wu, E., 2020. Squeeze-and-excitation networks. *IEEE Trans. Pattern Anal. Mach. Intell.* 42 (8), 2011–2023.

Jack, C.R., Bernstein, M.A., Fox, N.C., Thompson, P., Alexander, G., Harvey, D., Borowski, B., Britson, P.J., L. Whitwell, J., Ward, C., Dale, A.M., Felmlee, J.P., Gunter, J.L., Hill, D.L.G., Killiany, R., Schuff, N., Fox-Bosetti, S., Lin, C., Studholme, C., DeCarli, C.S., Gunnar Krueger, Ward, H.A., Metzger, G.J., Scott, K.T., Mallozzi, R., Blezek, D., Levy, J., Debbins, J.P., Fleisher, A.S., Albert, M., Green, R., Bartzokis, G., Glover, G., Mugler, J., Weiner, M.W., 2010. The Alzheimer's disease neuroimaging initiative(ADNI): MRI methods. *J. Magn. Reson. Imaging* 27 (4), 685–691.

Jack, C.R., Albert, M.S., Knopman, D.S., McKhann, G.M., Sperling, R.A., Carrillo, M.C., Thies, B., Phelps, C.H., 2011. Introduction to the recommendations from the National Institute on aging-Alzheimer's Association workgroups on diagnostic guidelines for Alzheimer's disease. *Alzheimer's Dement.* 7 (3), 257–262.

Jenkinson, M., Bannister, P., Brady, M., Smith, S., 2002. Improved optimization for the robust and accurate linear registration and motion correction of brain images. *Neuroimage* 17 (2), 825–841.

Klein, A., Andersson, J., Ardekani, B.A., Ashburner, J., Avants, B., Chiang, M.C., Christensen, G.E., Collins, D.L., Gee, J., Hellier, P., Song, J.H., Jenkinson, M., Lepage, C., Rueckert, D., Thompson, P., Vercauteren, T., Woods, R.P., Mann, J.J., Parsey, R.V., 2009. Evaluation of 14 nonlinear deformation algorithms applied to human brain MRI registration. *Neuroimage* 46 (3), 786–802.

Korolev S., Safullin A., Belyaev M., et al. Residual and plain convolutional neural networks for 3D brain MRI classification[C]//In Proceedings of the IEEE International Symposium on Biomedical Imaging, 2017.

Kossaiji J., Panagakis Y., Anandkumar A., et al. TensorLy: Tensor Learning in Python [C]//In Proceedings of the 30th Conference on Neural Information Processing Systems, 2016.

Lecun, Y., Bengio, Y., Hinton, G., 2015. Deep learning. *Nature* 521 (7553), 436–444.

Liu, M., Zhang, D., Shen, D., 2014. Hierarchical fusion of features and classifier decisions for Alzheimer's disease diagnosis. *Hum. Brain Mapp.* 35 (4), 1305–1319.

Lorenzi, M., Beltramello, A., Mercuri, N.B, et al., 2011. Effect of memantine on resting state default mode network activity in Alzheimer's disease. *Drugs Aging* 28 (3), 205–217.

Min, Lin, Qiang, Chen, Shuicheng, Yan, 2014. Network in network. *Proceedings of the IEEE International Conference on Learning Representations*, pp. 1305–1310.

Petersen, R.C., Aisen, P.S., Beckett, L.A., Donohue, M.C., Gamst, A.C., Harvey, D.J., Jack CR, Jr, Jagust, W.J., Shaw, L.M., Toga, A.W., Trojanowski, J.Q., Weiner, M.W., 2010. Alzheimer's Disease Neuroimaging Initiative(ADNI): clinical characterization. *Neurology* 74 (3), 201–209.

Ridnik, T., Lawen, H., Noy, A., et al., 2020. TRResNet: high performance GPU-dedicated architecture[DB/OL]. arXiv:2003. 13630.

Roberts, R., Knopman, D.S., 2013. Classification and epidemiology of MCI. *Clin. Geriatr. Med.* 29 (4), 753–772.

Servick, K., 2019. Another major drug candidate targeting the brain plaques of Alzheimer's disease has failed. What's left? *Science*.

Taqi, A.M., Awad, A., Al-Azzo, F., Milanova, M., 2018. The impact of multi-optimizers and data augmentation on tensor flow convolutional neural network performance. *Proceedings of the IEEE Conference on Multimedia Information Processing and Retrieval*, pp. 140–145.

Valliani, A., Soni, A., 2017. Deep residual nets for improved Alzheimer's diagnosis. *Proceedings of the 8th ACM International Conference on Bioinformatics, Computational Biology, and Health Informatics*, p. 615.

Vincent, P., Larochelle, H., Lajoie, I., et al., 2010. Stacked denoising autoencoders: learning useful representations in a deep network with a local denoising criterion. *J. Mach. Learn. Res.* 11 (12), 3371–3408.

Vu, T.D., Ho, N.H., Yang, H.J., Kim, J., Song, H.C., 2018. Non-white matter tissue extraction and deep convolutional neural network for Alzheimer's disease detection. *Soft Comput.* 22, 6825–6833.

Wang, S., Shen, Y., Wei, C., et al., 2017. Automatic recognition of mild cognitive impairment from MRI images using expedited convolutional neural networks. *Proceedings of the International Conference on Artificial Neural Networks*. Springer, Cham.

Wen, J., Thibeau-Sutre, E., Diaz-Melo, M., Samper-González, J., Routier, A., Bottani, S., Dormont, D., Durrleman, S., Burgos, N., Colliot, O., 2020. Convolutional neural networks for classification of Alzheimer's disease: overview and reproducible evaluation. *Med. Image Anal.* 63, 101694.

Wood, D., Cole, J., Booth, T., 2019. NEURO-DRAM: a 3D recurrent visual attention model for interpretable neuroimaging classification[DB/OL]. arXiv:1910. 04721.

- Woolrich, M.W., Jbabdi, S., Patenaude, B., Chappell, M., Makni, S., Behrens, T., Beckmann, C., Jenkinson, M., Smith, S.M., 2009. Bayesian analysis of neuroimaging data in FSL. *Neuroimage* 45 (1), S173–S186.
- Wu, C., Guo, S., Hong, Y., Xiao, B., Wu, Y., Zhang, Q., Alzheimer's Disease Neuroimaging, I., 2018. Discrimination and conversion prediction of mild cognitive impairment using convolutional neural networks. *Quant. Imaging Med. Surg.* 8, 992–1003.
- Zhan, L., Zhou, J., Wang, Y., Jin, Y., Jahanshad, N., Prasad, G., Nir, T.M., Leonardo, C.D., Ye, J., Thompson, P.M., For The Alzheimer's Disease Neuroimaging, I., 2015. Comparison of nine tractography algorithms for detecting abnormal structural brain networks in Alzheimer's disease. *Front. Aging Neurosci.* 7, 48.
- Zhang, L., Wang, M., Liu, M., Zhang, D., 2020. A survey on deep learning for neuroimaging-based brain disorder analysis. *Front. Neurosci.* 14, 779.